Persoonia 46, 2021: 116–128
www.ingentaconnect.com/content/nhn/pimj

RESEARCH ARTICLE

ISSN (Online) 1878-9080
https://doi.org/10.3767/persoonia.2021.46.04

Genome-scale phylogenies reveal relationships among *Parastagonospora* species infecting domesticated and wild grasses

D. Croll[1], P.W. Crous[2,3], D. Pereira[4,5,6], E.A. Mordecai[7], B.A. McDonald[4,*], P.C. Brunner[4]

Key words

host range
leaf and glume blotch of wheat
new taxa
pathogen emergence
taxonomy

Abstract Several plant pathogenic *Parastagonospora* species have been identified infecting wheat and other cereals over the past 50 years. As new lineages were discovered, naming conventions grew unwieldy and the relationships with previously recognized species remained unclear. We used genome sequencing to clarify relationships among these species and provided new names for most of these species. Six of the nine described *Parastagonospora* species were recovered from wheat, with five of these species coming from Iran. Genome sequences revealed that three strains thought to be hybrids between *P. nodorum* and *P. pseudonodorum* were not actually hybrids, but rather represented rare gene introgressions between those species. Our data are consistent with the hypothesis that *P. nodorum* originated as a pathogen of wild grasses in the Fertile Crescent, then emerged as a wheat pathogen via host-tracking during the domestication of wheat in the same region. The discovery of a diverse array of *Parastagonospora* species infecting wheat in Iran suggests that new wheat pathogens could emerge from this region in the future.

Citation: Croll D, Crous PW, Pereira D, et al. 2021. Genome-scale phylogenies reveal relationships among Parastagonospora species infecting domesticated and wild grasses. Persoonia 46: 116–128. https://doi.org/10.3767/persoonia.2021.46.04.
Effectively published online: 14 February 2021 [Received: 1 December 2020; Accepted: 19 January 2021].

INTRODUCTION

Parastagonospora nodorum is an important wheat pathogen with a global distribution. It has been subjected to intensive population genetic analyses using a variety of genetic markers, including RFLPs in nuclear and mitochondrial genomes (Keller et al. 1997, Sommerhalder et al. 2007), microsatellites (SSRs; Stukenbrock et al. 2006), sequences of genes encoding important traits like virulence (Stukenbrock et al. 2007b, Ghaderi et al. 2020) and fungicide sensitivity (Pereira et al. 2017) as well as entire genome sequences (Richards et al. 2019, Pereira et al. 2020a, c). These studies revealed that *P. nodorum* populations are characterized by regular recombination, high levels of gene flow, high effective population sizes, and varying frequencies of effector genes encoding host-selective toxins (McDonald et al. 2013). Analyses of several field populations from Iran indicated that *P. nodorum* most likely originated in the Fertile Crescent (McDonald et al. 2012, Ghaderi et al. 2020), the same region where wheat was domesticated (Salamini et al. 2002), providing support for the hypothesis that this pathogen emerged through host-tracking (Stukenbrock et al. 2008). Analyses of DNA sequences revealed that several different *Parastagonospora* lineages can be found on wheat in Iran, including one species that was also found infecting wheat in other geographical regions, as well as new lineages that had not previously been found on wheat (McDonald et al. 2012). Some lineages were also suspected to be of hybrid origin (McDonald et al. 2012), which suggested there may be significant uncertainty associated with resolving phylogenetic relationships among these lineages based on a small number of gene sequences. Here, we used genome sequences to identify thousands of orthologous gene sequences to build a phylogenomic tree among these wheat-infecting species and place them into a larger context that includes *Parastagonospora* species found on wild grasses in the Fertile Crescent and other continents (Appendix).

The different pathogens in the *Parastagonospora* complex (previously *Phaeosphaeria*) causing cereal diseases were originally defined based on spore morphology, host specialization and the formation of sexual ascomata (Shaw 1957a, b). Isolates that were most aggressive on wheat and showed heterothallic mating type behaviour formed the group now called *P. nodorum*. Isolates collected from oats or other hosts were initially named *Leptosphaeria avenaria*, with the species name reflecting the host preference. Subsequent DNA-based analyses supported placing this group into the *Phaeosphaeriaceae* and it was renamed *Phaeosphaeria avenaria*. A third group of isolates were morphologically similar to *P. avenaria*, but were not able to infect

[1] Laboratory of Evolutionary Genetics, Institute of Biology, University of Neuchâtel, CH-2000 Neuchâtel, Switzerland.
[2] Westerdijk Fungal Biodiversity Institute, Uppsalalaan 8, 3584 CT Utrecht, The Netherlands.
[3] Wageningen University and Research Centre (WUR), Laboratory of Phytopathology, Droevendaalsesteeg 1, 6708 PB Wageningen, The Netherlands.
[4] Plant Pathology Group, Institute of Integrative Biology, ETH Zurich, Universitätstrasse 2, CH-8092 Zurich, Switzerland; corresponding author e-mail: bruce.mcdonald@usys.ethz.ch.
[5] Environmental Genomics, Max Planck Institute for Evolutionary Biology, 24306, Plön, Germany.
[6] Environmental Genomics, Christian-Albrechts University of Kiel, 24118, Kiel, Germany.
[7] Biology Department, Stanford University, 327 Campus Drive, Stanford, California, 94305 USA.

oats, instead being weakly aggressive on wheat. This group was named *Phaeosphaeria avenaria* f. sp. *tritici* (*Pat*) (Ueng et al. 1995). Further analyses that provided additional evidence for host specialization (Martin & Cooke 1979, Osbourn et al. 1986, Cunfer & Ueng 1999) and genetic differences between host specialized forms (Ueng & Chen 1994, Ueng et al. 1998, Malkus et al. 2005) led to splitting *Pat* into three groups called *Pat-1*, *Pat-2* and *Pat-3*. These early phylogenetic studies, which often relied on analyzing a single genetic locus and a small number of isolates, gave inconsistent results.

A more recent study (McDonald et al. 2012) that included more than 350 globally distributed *Parastagonospora* strains and sequences of five different genes (both mating type loci, ITS, B-tubulin and B-xylosidase) led to the discovery of new *Pat* lineages infecting other grass species in Iran and North America. This dataset also identified 14 strains in Canada and Iran that appeared to be hybrids between *Pat-1* and *P. nodorum*, suggesting that species boundaries may be permeable. The Iranian wheat fields were colonized mainly by *P. nodorum* and *Pat-1*, but also by two other *Parastagonospora* species identified earlier (McDonald et al. 2012) and a new species discovered in this analysis. A recent study used ITS sequences to identify a clade of *Parastagonospora* strains infecting native *Stipa pulchra* grass in California (Spear & Mordecai 2018). The affiliation of this clade to the other *Parastagonospora* species found on grasses was not known, but we hypothesized that this species may have emerged through the mechanism of 'spill-back', where a pathogen specialized to infect a host – often a domesticated host – in one location is introduced into a new location and becomes adapted to a new host – often a native, wild species (Kelly et al. 2009). An example of spill-back in plant pathology is the adaptation of *Rhynchosporium graminicola* to infect wild barley (*Hordeum spontaneum*) in northern Africa thousands of years after its emergence as a pathogen of cultivated barley (*Hordeum vulgare*) in northern Europe (Kiros-Meles et al. 2011).

We utilized a genome-scale dataset and a wide array of *Parastagonospora* species to explore the phylogenetic relationships among these species and to better define the species boundaries. Based on our findings, we propose names for seven new *Parastagonospora* species. We also sought to determine whether the putative *Pat-1*/*P. nodorum* hybrid strains identified based on analyzing five genes were truly hybrids. Finally, we explored the hypothesis that the *Parastagonospora* strains found on wild *Stipa* could have originated via spill-back from *P. nodorum* strains infecting wheat in California.

MATERIALS AND METHODS

Isolates

Twenty-two of the analyzed *Parastagonospora* strains were isolated from wheat, including four strains originating from global collections of *P. nodorum* that were already analyzed for both phenotypes and entire genome sequences (Pereira et al. 2020a, b, c). Seven strains came from other grass hosts and had previously been analyzed using a limited number of conserved gene sequences (McDonald et al. 2012), but had not previously been genome sequenced. We included representatives of most of the known *Phaeosphaeria avenaria* f. sp. *tritici* (*Pat*) clades that were identified by plant pathologists over the last three decades. *Parastagonospora stipae* isolates were obtained from wild *Stipa pulchra* in the Jasper Ridge Biological Preserve, San Mateo County, California during a survey of naturally occurring foliar fungal pathogens in the summer of 2015 (Spear & Mordecai 2018). A summary of the isolates included in these analyses is shown in Table 1.

For strains included in morphological analyses, single conidial colonies were established by excising 2 × 2 mm tissue pieces from the leading margin of disease, surface sterilizing them in sequential baths of alcohol and bleach, and plating it onto 2 % malt extract agar (MEA) with chloramphenicol. These isolates were then sub-cultured to obtain axenic cultures. Cultures were maintained in Petri dishes sealed with parafilm at room temperature in the laboratory. Colonies were sub-cultured on 2 % potato-dextrose agar (PDA), oatmeal agar (OA), MEA, autoclaved *Triticum* and *Hordeum* seed and leaves on synthetic nutrient-poor agar (SNA) (Crous et al. 2019), and incubated at 25 °C under continuous near-ultraviolet light to promote sporulation. Reference strains and specimens of the studied fungi are maintained in the CBS culture collection (CBS) of the Westerdijk Fungal Biodiversity Institute (WI), Utrecht, the Netherlands.

Culturing, DNA extraction, and whole-genome sequencing

All isolates were initially established from single-spore isolations. Four-day-old colonies growing on PDA media were harvested for mycelial fragments and transferred to 50 mL Potato Dextrose Broth (PDB) media. The transferred fragments were cultured 4–6 d at 24 °C at 120 rpm. Sterile cheesecloth was used for filtering and the fungal material was then lyophilized at room temperature for 72 h. DNA extractions were performed from dried material with the DNeasy Plant Mini Kit (Qiagen) following the manufacturer's protocol. Genomic DNA was sequenced on the Illumina HiSeq 2500 platform with a paired-end 100 bp cycle protocol. Library preparation and sequencing was performed by the Functional Genomics Center Zurich (FGCZ). Raw sequence reads were deposited in the NCBI Sequence Read Archive (SRA) under the BioProject PRJNA606320 (Pereira et al. 2020a, c). Sequencing reads of additional genomes were retrieved from BioProject accessions SRP155908, SRP159197 (Syme et al. 2018, Richards et al. 2019).

Genome assembly and gene annotation

Draft genome assemblies were produced for each isolate using SPAdes v. 3.14.1 (Bankevich et al. 2012) with the --careful option and a pre-determined kmer range of 21,33,55,66,99,127 (the latter kmer was omitted if the read length was 100 bp). Assemblies were quality checked using Quast v. 5.0.2 (Gurevich et al. 2013). To train accurate gene predictions, RNAseq data from the *P. nodorum* reference genome strain SN15 was retrieved from the NCBI Sequence Read Archive (Jones et al. 2019). The datasets SRR11785359, SRR11785360, SRR11785362 matching the wild-type genotype of SN15 were used. All transcriptomic reads were aligned to the reference genome of *P. nodorum* SN15 (Hane et al. 2007) using STAR v. 2.7.5a (Dobin et al. 2013). bam2hints included in Augustus v. 3.3.3 was used to retrieve intron splice site hints and filtered for a minimum read support of 10 (Stanke & Morgenstern 2005). Intron splice site hints were used for a comprehensive gene model training using Braker v. 2.1.5 including GeneMark-ET and Augustus v. 3.3.3 (Stanke & Morgenstern 2005, Hoff et al. 2019). After successful gene model training, Augustus v. 3.3.3 was used to annotate all assembled genomes with '--alternatives-from-evidence=false' and '--UTR=off'. Predicted protein sequences were retrieved from each genome for downstream analyses.

Orthology analyses of maximum-likelihood tree reconstruction

Orthology relationships were established among all assembled genomes as well as genomes from representative ascomycetes retrieved from Fungal Ensembl Genome (release 47) using a script provided by G. Leonard (https://github.com/guyleonard/get_jgi_genomes). Sets of protein sequences were used for pairwise BLAST analyses and ortholog reconstruction using

Table 1 *Parastagonospora* isolates that were included in phylogenetic analyses. All isolates were analyzed using complete genome sequences except for the three *P. stipae* strains that were analyzed using five AFTOL genes. NCBI GenBank or Sequence Read Archive (SRA) accession numbers are provided.

Species	Original accession no. (original species name, associated publication)	Culture collection no.[1]	Geographical origin	Host	Collector	Year	NCBI GenBank / SRA accession
P. arcana	IR_G2.1A (*P. nodorum*, McDonald et al. 2012)	CPC 36218, CBS 146965	Iran	*Triticum aestivum* leaf	M. Razavi	2005	SRR11074990
P. avenae	BARKER (*Parastagonospora avenaria*, McDonald et al. 2012)	CPC 36201, CBS 146876	Australia	*Avena sativa*	K. Clarke	2009	SRR11075041
	NY_391 (*P. nodorum*, Stukenbrock et al. 2006)	CPC 36222	New York USA	*Triticum aestivum*	G. Bergstrom	1991	SRR11075100
P. bromicola	83.6011.2 (*Pat-5*, McDonald et al. 2012)	CPC 36214, CBS 146870	North Dakota USA	*Bromus inermis*	J. Krupinsky	1983	SRR11075116
	82.4841 (*Pat-5*, McDonald et al. 2012)		North Dakota USA	*Bromus inermis*	J. Krupinsky	1983	SRR11075117
P. dactylidigena	IR_2_1.1 (*Pat-4*, McDonald et al. 2012)		Iran	*Dactylis glomerata*	M. Razavi	2011	SRR11075010
	IR_2_5.2 (*Pat-4*, McDonald et al. 2012)	CPC 36213, CBS 146869	Iran	*Dactylis glomerata*	M. Razavi	2011	SRR11075003
P. golestanensis	IR_7_2.3 (*Pat-6*, McDonald et al. 2012)		Iran	*Dactylis glomerata*	M. Razavi	2011	SRR11075005
	IR_6_1.1 (*Pat-6*, McDonald et al. 2012)	CPC 36217, CBS 146871	Iran	*Agropyron tauri*	M. Razavi	2011	SRR11075004
P. jasniorum	IR_A1_3.1A (*P-2*, McDonald et al. 2012)	CPC 36200, CBS 146866	Iran	*Triticum aestivum* leaf	M. Razavi	2005	SRR11075006
	IR_H6.2B (*P-2*, McDonald et al. 2012)		Iran	*Triticum aestivum* leaf	M. Razavi	2005	SRR11075007
P. nodorum	IR_B2.1B (*P. nodorum*, McDonald et al. 2012)	CPC 36202, CBS 146873	Iran	*Triticum aestivum* leaf	M. Razavi	2005	SRR11074999
	IR_2.1A (*P. nodorum*, McDonald et al. 2012)		Iran	*Triticum aestivum* seed	M. Razavi	2010	SRR11075002
	CASSILS (*Pat-1*/*P. nodorum* hybrid, McDonald et al. 2012)		Canada	*Triticum aestivum* seed	R. Clear	2005	SRR11075038
	SA 10 (*P. nodorum*, Pereira et al. 2020a)		South Africa	*Triticum aestivum* leaf	Z. Pretorius	2007	SRR11074975
	CH 1A9A (*P. nodorum*, Pereira et al. 2020a)		Switzerland	*Triticum aestivum* leaf	S. Keller	1994	SRR11075141
	AUS 1A3 (*P. nodorum*, Pereira et al. 2020a)		Australia	*Triticum aestivum* leaf	B. McDonald	2001	SRR11075148
	TX_XA2.1 (*P. nodorum*, Pereira et al. 2020a)		United States	*Triticum aestivum* leaf	B. McDonald	1992	SRR11075068
P. pseudonodorum	AYLSHAM (*Pat-1*, McDonald et al. 2012)		Canada	*Triticum aestivum* seed	R. Clear	2005	SRR11075040
	BRIERCREST (*Pat-1*, McDonald et al. 2012)		Canada	*Triticum aestivum* seed	R. Clear	2005	SRR11075039
	IR_5.2B (*Pat-1*, McDonald et al. 2012)	CPC 36208, CBS 146867	Iran	*Triticum aestivum* seed	M. Razavi	2010	SRR11075009
	JANSEN4 (*Pat-1*/*P. nodorum* hybrid, McDonald et al. 2012)		Canada	*Triticum aestivum* seed	R. Clear	2005	SRR11075037
	HARTNEY (*Pat-1*/*P. nodorum* hybrid, McDonald et al. 2012)		Canada	*Triticum aestivum* seed	R. Clear	2005	SRR11075036
P. stipae	Mordecai_1418	CPC 36223, CBS 146872	California USA	*Stipa pulchra* leaf	E. Mordecai and E. Spear	2015	MW263182 MW263179 MW263168 MW263174 MW263171
	Mordecai_1617		California USA	*Stipa pulchra* leaf	E. Mordecai and E. Spear	2015	MW263184 MW263181 MW263170 MW263176 MW263173
	Mordecai_1522		California USA	*Stipa pulchra* leaf	E. Mordecai and E. Spear	2015	MW263183 MW263180 MW263169 MW263175 MW263172
P. zildae	IR_B4.2A (*P-1*, McDonald et al. 2012)	CPC 36198, CBS 146864	Iran	*Triticum aestivum* leaf	M. Razavi	2005	SRR11075008
	IR_H4.1A (*P-1*, McDonald et al. 2012)		Iran	*Triticum aestivum*, leaf	M. Razavi	2005	SRR11074987
	IR_C2.2B		Iran	*Triticum aestivum*, leaf	M. Razavi	2005	SRR11074976
	IR_C2.2A	CPC 36221, CBS 146865	Iran	*Triticum aestivum*, leaf	M. Razavi	2005	SRR11074977

[1] CBS: Westerdijk Fungal Biodiversity Institute, Utrecht, The Netherlands; CPC: Culture collection of Pedro Crous, housed at CBS.

Orthofinder v. 2.4.0 (Emms & Kelly 2019). The default inflation index of 1.5 was used and set the sequence alignment procedure to 'msa', which uses mafft with --maxiterate 1000 to generate sequence alignments of each orthogroup (Katoh & Standley 2013). A concatenated alignment was retrieved of all single-copy orthogroups (n = 2425) with a minimum of 98.0 % of species having single-copy genes in any orthogroup. Maximum likelihood tree searches were performed with a randomized parsimony starting tree, a general time reversible (GTR) protein model with unequal rates and unequal base frequencies using raxml-ng 0.9.0 (Kozlov et al. 2019). Felsenstein bootstrap replicates (n = 100) were performed and the final tree was produced using ggtree (Yu 2020).

Sequencing of fungal barcoding genes, cleaning, concatenation and phylogeny

Primers for the AFTOL (Assembling the Fungal Tree of Life) genes (ITS, LSU, *RPB1*, *RPB2*, *TEF1*) were designed using the software Primer3 (Untergasser et al. 2012) based on the reference genome of the SN15 isolate (Hane et al. 2007). The genes were amplified in *P. stipae* isolates with conditions for PCR amplification as follows: 96 °C for 2 min, 35 cycles at 96 °C for 30 s, 56 °C for 30 s, 72 °C for 1 min, and a final step at 72 °C for 5 min. Amplified products were purified using manufacturer protocols for illustra Sephadex G-50 fine DNA Grade Column (GE Healthcare, Pittsburgh, USA) and sequenced in an ABI 3130xl Genetic Analyzer (Life Technologies, Applied Biosystems). Raw Sanger sequence reads of each primer were checked for quality and assembled into final gene sequences using Geneious v. 9.1.8 (Biomatters, Auckland, New Zealand). Gene sequences for ITS, LSU, *RPB2* and *TEF1* were available for *P. phragmitis* and *P. novozelandica* (Marin-Felix et al. 2019). Nucleotide sequences for the remaining species were extracted from the genome sequences available. Final datasets were obtained after a concatenation step using the MAFFT online tool v. 7.0 (Katoh et al. 2019). The concatenated dataset files were used to reconstruct maximum likelihood trees also in RaxML v. 8.0 (Stamatakis 2014).

Morphology

Representative strains were morphotyped for a series of morphological characters. Slide preparations were mounted in Shear's mounting fluid from colonies sporulating on MEA, PDA, OA or leaf tissue on SNA. Observations were made with a Nikon SMZ25 dissection-microscope, and with a Zeiss Axio Imager 2 light microscope using differential interference contrast (DIC) illumination and images recorded on a Nikon DS-Ri2 camera with associated software. Colony characters and pigment production were noted after 2–4 wk of growth on MEA, PDA and OA (Crous et al. 2019) incubated at 25 °C. Colony colours (surface and reverse) were scored using the colour charts of Rayner (1970).

RESULTS

The genome-scale tree resolved nine distinct *Parastagonospora* species (Fig. 1). *Parastagonospora nodorum* isolates from wheat fields on four continents (Africa, North America, Europe, Australia) formed a single well-resolved clade that was most closely related to *P. pseudonodorum* (previously named *Pat-1*), *P. bromicola* (previously *Pat-5*), *P. dactylidigena* (previously *Pat-4*) and *P. avenae* (previously *Phaeosphaeria avenaria*). Considerable differences were found between the two *P. avenae* strains, which may reflect additional cryptic species in this clade. More distant from *P. nodorum* were *P. golestanensis* (previously *Pat-6*), *P. zildae* (previously *P-1*), *P. jasniorum* (previously *P-2*) and *P. arcana*. Five of these species (*P. arcana*, *P. jasniorum*, *P. nodorum*, *P. pseudonodorum*,

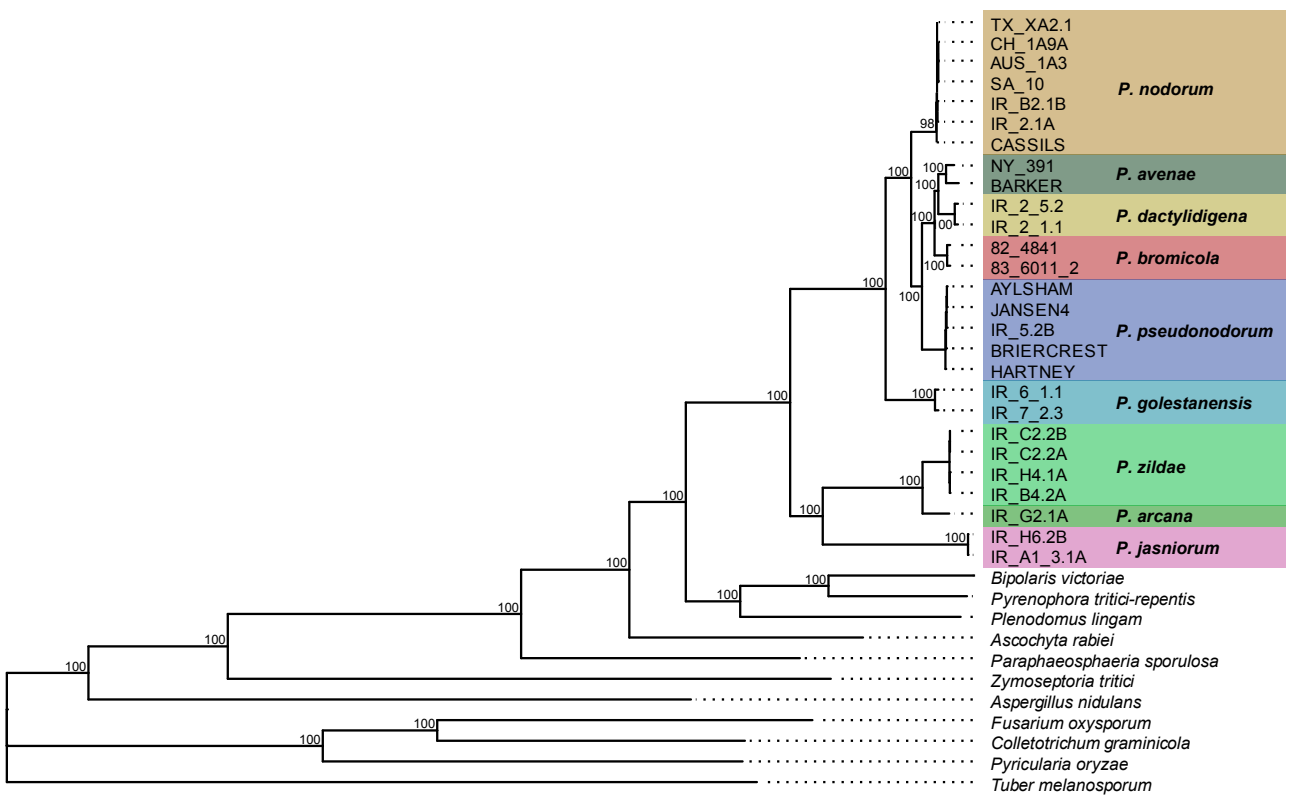

Fig. 1 Maximum likelihood phylogenomic tree generated from a concatenated alignment of sets of orthologous protein sequences retrieved from *Parastagonospora* draft genomes and representative ascomycetes. A total of 2425 single-copy orthologs with ≥ 98.0 % of the species included were retained. The tree was estimated based on the general time reversible (GTR) protein model and branch support corresponds to Felsenstein bootstrap values (n = 100). Bootstrap values below 98 % were omitted. The root was defined as the node connecting *Tuber melanosporum*. Genome sequences outside of the *Parastagonospora* genus were retrieved from Ensembl Fungi (https://fungi.ensembl.org/index.html).

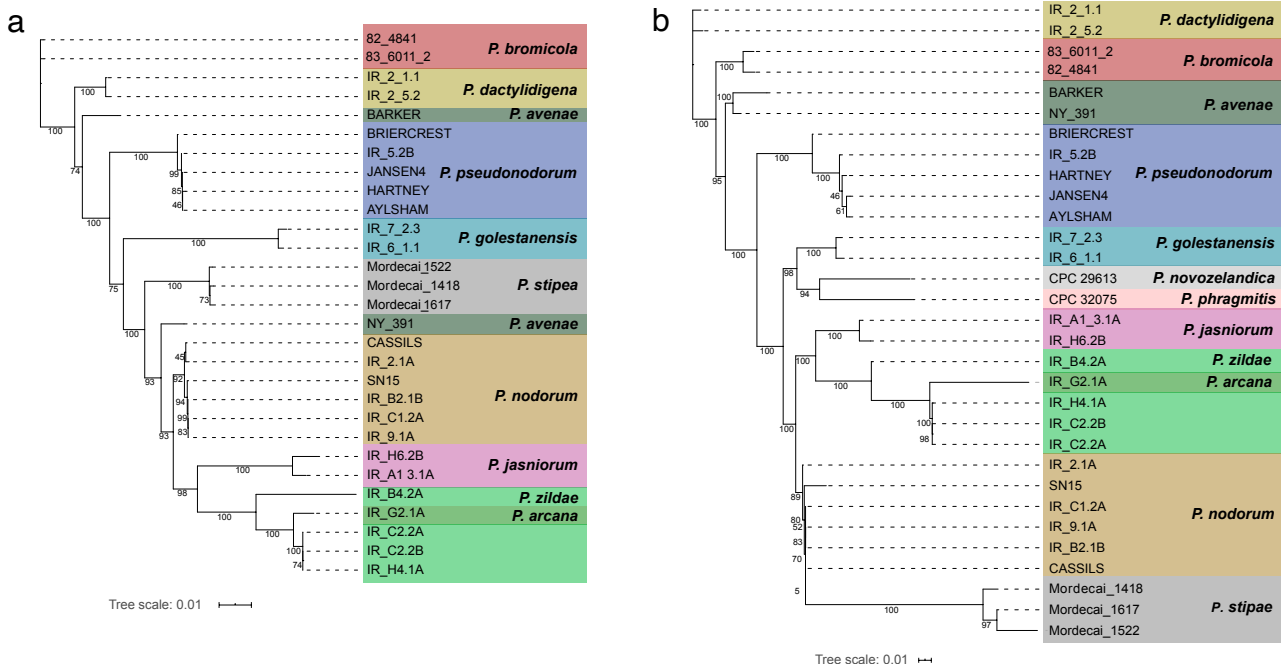

Fig. 2 Maximum likelihood phylogenetic trees. a. Phylogenetic tree generated from a concatenated alignment of ITS, LSU, *RPB1*, *RPB2* and *TEF1a* nucleotide sequences that include *Parastagonospora stipae*; b. phylogenetic tree generated from a concatenated alignment of ITS, LSU, *RPB2* and *TEF1* sequences that includes *Parastagonospora phragmitis* and *P. novozelandica*.

P. zildae) were found infecting wheat in Iran and *P. avenae* was found infecting wheat in North America, indicating that at least six species in the *Parastagonospora* clade can infect wheat.

Because we did not obtain genome sequences for any of the *P. stipae* isolates, we constructed a new phylogenetic tree using concatenated ITS, LSU, *RPB1*, *RPB2* and *TEF1a* sequences for all of the *Parastagonospora* species (Fig. 2a). Many of the species relationships indicated in the genome-scale phylogenetic tree were also found in the tree based on these five AFTOL genes. This tree indicated that *P. stipae* was distinct from the other species, but was most closely related to *P. avenae*.

Parastagonospora phragmitis and *P. novozelandica* are two recently described *Parastagonospora* species infecting wild grasses in Australia and New Zealand, respectively (Marin-Felix et al. 2019). Their relationship to the nine *Parastagonospora* species described here was determined based on concatenated ITS, LSU, *RPB2*, *TEF1a* sequences (Fig. 2b). Many of the species relationships indicated in the genome-scale phylogenetic tree were also found in the tree based on these four AFTOL genes. This tree indicated that *P. phragmitis* and *P. novozelandica* were separate species that were most closely related to *P. golestanensis*, while *P. stipae* was most closely related to *P. nodorum* and a *P. avenae* strain isolated from wheat in New York.

Taxonomy

Based on morphology and a multi-locus phylogeny of the isolates studied, nine *Parastagonospora* species are recognized, of which seven are newly described. In total, 26 species of *Parastagonospora* are presently known from DNA sequence data (Appendix).

Parastagonospora arcana B.A. McDonald, P.C. Brunner, Croll, D. Pereira & Crous, *sp. nov.* — MycoBank MB838010; Fig. 3

Etymology. *arcanus* = secret or mystery, reflecting the fact that this species was previously assumed to be *P. nodorum*.

Typus. Iran, Golestan Province, on infected glume of *Triticum aestivum*, 2005, *M. Razavi* (holotype CBS H-24479, cultures ex-type CPC 36218 = IR_G2.1A = CBS 146965).

Ascocarps pseudothecial, solitary, erumpent, globose, brown to dark brown, 200–250 µm diam; wall of 3–6 layers of brown

Fig. 3 *Parastagonospora arcana* (CPC 36221). a. Ascomata developing on PDA; b–d. asci, ascospores and pseudoparaphyses. — Scale bars: a = 250 µm, all others = 10 µm.

textura angularis; ostiole central, not to slightly papillate. *Asci* 70–95 × 8–10 µm, bitunicate, subcylindrical, straight to slightly curved, short stipitate, 8-spored, with well-defined apical chamber, 1–1.5 µm diam. *Pseudoparaphyses* filiform, hyaline, septate, hyphae-like, unbranched, rarely anastomosing, 2–2.5 µm diam. *Ascospores* bi- to triseriate in asci, fusoid, guttulate, pale brown, smooth, widest in penultimate cell, becoming slightly constricted at septa with age, (24–)25–28(–32) × (4–)5(–5.5) µm, 5-septate.

Cultural characteristics — Colonies covering dish after 2 wk at 25 °C in the dark, smooth, with even margin, and moderate to fluffy aerial mycelium. On MEA surface pale olivaceous grey, reverse isabelline; on PDA surface pale olivaceous grey, reverse isabelline; on OA surface pale olivaceous grey.

Notes — *Parastagonospora arcana* is sister to *P. zildae* (98.4 % identity based on ITS) and confirmed as distinct based on the multigene dataset. Both species only produced a sexual morph in culture. Morphologically, the two species are very similar, and are best distinguished based on their DNA data.

Parastagonospora avenae (A.B. Frank) Quaedvlieg et al., Stud. Mycol. 75: 362. 2013 — Fig. 4

Basionym. *Septoria avenae* A.B. Frank, Ber. Deutsch. Bot. Ges. 13: 64. 1895.

Synonyms. *Stagonospora avenae* (A.B. Frank) Bissett (as '*avena*'), Fungi Canadenses, Ottawa 239: 1. 1982.

Leptosphaeria avenaria G.F. Weber, Phytopathology 12: 449. 1922.

Phaeosphaeria avenaria (G.F. Weber) O.E. Erikss., Ark. Bot., Ser. 2 6: 408. 1967.

Pleospora tritici Garov., Arch. Triennale Lab. Bot. Crittog. 1: 123. 1874.

Spermatogonia solitary to aggregated, globose, brown, 60–90 µm diam with central ostiole; wall of 3–6 layers of brown *textura angularis*. *Spermatophores* reduced to spermatogenous cells. *Spermatogenous cells* hyaline, smooth, ampulliform, 7–10 × 3–5 µm, with indistinct apical percurrent proliferation. *Spermatia* solitary, hyaline, smooth, guttulate, subcylindrical with obtuse apex and truncate base, aseptate, 4–6 × 2 µm.

Culture characteristics — Colonies flat, spreading, reaching 60 mm diam after 2 wk, with moderate aerial mycelium, and even, smooth margins. On MEA, PDA and OA surface and reverse ochreous.

Material examined. Australia, Mt Barker, on *Avena sativa*, 2009, *K. Clarke*, specimen CBS H-2439, culture CPC 36201 = avenaria_BARKER = CBS 146876.

Notes — Bissett (1982) noted that conidia *in vivo* can be (1–)3(–7)-septate, 17–46 × 2.6–4.4 (av. 33 × 3.5) µm in size. Unfortunately, no conidiomata were observed in culture as the present strain only formed spermatogonia.

Parastagonospora bromicola B.A. McDonald, P.C. Brunner, Croll, D. Pereira & Crous, *sp. nov.* — MycoBank MB838011; Fig. 5

Etymology. Name reflects the host genus it was isolated from, *Bromus*.

Typus. USA, North Dakota, on *Bromus inermis*, 1983, *J. Krupinsky*, USDA-ARS (holotype CBS H-24387, cultures ex-type CPC 36214 = Pat-5 83.6011.2 = CBS 146870).

Conidiomata solitary, pycnidial, dark brown to black, globose, 150–200 µm diam, with central ostiole; wall with 3–6 layers of pale brown *textura angularis*. *Conidiophores* reduced to conidiogenous cells lining the inner cavity. *Conidiogenous cells* hyaline, smooth, ampulliform to subcylindrical, 4–6 × 4–5 µm, proliferating percurrently at apex. *Conidia* solitary, hyaline, smooth, guttulate, subcylindrical, straight to slightly curved, apex subobtuse, base truncate, 2 µm diam, 1(–3)-septate, (12–)14–16(–18) × (2–)2.5–3 µm.

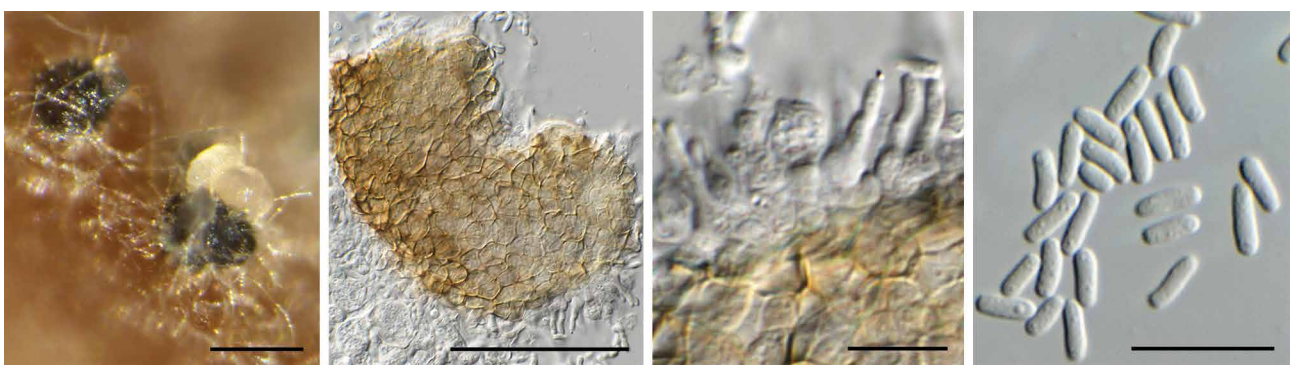

Fig. 4 *Parastagonospora avenae* (CPC 36201). a. Conidiomata developing on PDA; b. conidiomal wall with conidiogenous cells; c. close-up of conidiogenous cells giving rise to conidia; d. conidia. — Scale bars: a = 100 µm, b = 50 um, c–d = 10 µm.

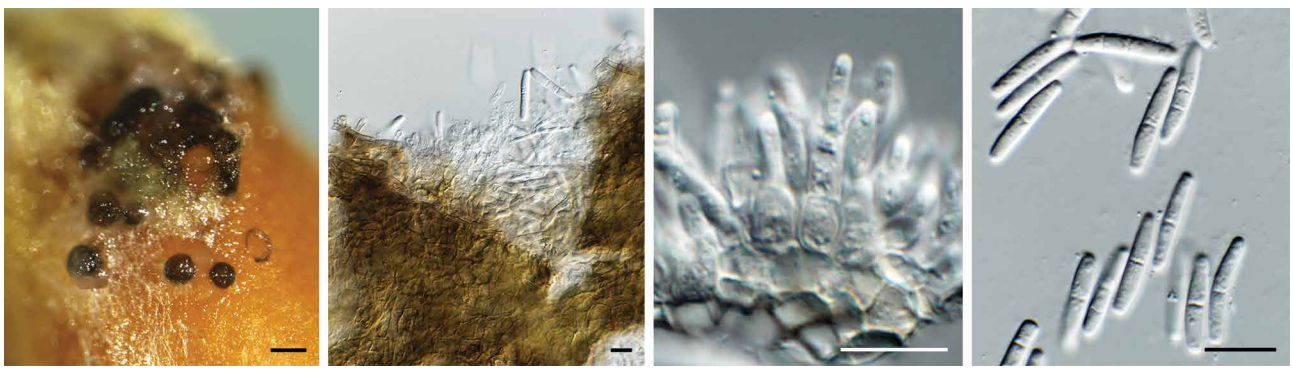

Fig. 5 *Parastagonospora bromicola* (CPC 36214). a. Conidiomata developing on PDA; b. conidioma with oozing conidia; c. conidiogenous cells giving rise to conidia; d. conidia. — Scale bars: a = 200 µm, all others = 10 µm.

Culture characteristics — Colonies flat, spreading, covering dish after 2 wk, with moderate aerial mycelium, and even, lobate margins. On MEA surface luteous, reverse ochreous; on PDA surface smoke grey, outer region olivaceous grey, reverse olivaceous grey; on OA surface saffron.

Notes — *Parastagonospora bromicola* occurs on *Bromus*, and has smaller conidia than are commonly associated with taxa in the *P. nodorum* complex.

Parastagonospora dactylidigena B.A. McDonald, P.C. Brunner, Croll, D. Pereira & Crous, *sp. nov.* — MycoBank MB838012; Fig. 6

Etymology. Name reflects the host genus it was isolated from, *Dactylis.*

Typus. Iran, Golestan Province, on *Dactylis glomerata*, 2011, *M. Razavi* (holotype CBS H-24386, cultures ex-type CPC 36213 = Pat-4 IR_2_5.2 = CBS 146869).

Conidiomata solitary, pycnidial, brown, globose, 250–350 µm diam, with central ostiole; wall with 3–6 layers of pale brown *textura angularis. Conidiophores* reduced to conidiogenous cells lining the inner cavity. *Conidiogenous cells* hyaline, smooth, ampulliform to subcylindrical, 5–7 × 4–5 µm, proliferating percurrently at apex. *Conidia* solitary, hyaline, smooth, guttulate, subcylindrical, straight to slightly curved, apex subobtuse, base truncate, 2.5–3.5 µm diam, 3(–6)-septate, (25–)30–37(–42) × 4(–5) µm.

Culture characteristics — Colonies flat, spreading, covering dish after 2 wk, with moderate aerial mycelium, and even, lobate margins. On MEA surface luteous buff, reverse orange; on PDA surface luteous buff, reverse saffron; on OA surface luteous buff.

Notes — Li et al. (2015) described several species of *Parastagonospora* from *Dactylis* collected in Italy, namely *P. allouniseptata* (conidia 1-septate, 16–22 × 2.5–3.5 µm), *P. dactylidigena* (conidia 3-septate, 25–40 × 4–5.5 µm), *P. minima* (conidia 3-septate, 20–28 × 3.5–4.5 µm) and *P. italica* (conidia 3-septate, 25–32 × 3–4 µm). An additional three sexual species were subsequently described from this host, namely *P. campignensis* (Li et al. 2016), *P. fusiformis* and *P. poaceicola* (Thambugala et al. 2017). *Parastagonospora dactylidigena* which also occurs on *Dactylis*, is phylogenetically distinct, and morphologically easily distinguished from these taxa and those in the *P. nodorum* complex, based its multiseptate, longer conidia.

Parastagonospora golestanensis B.A. McDonald, P.C. Brunner, Croll, D. Pereira & Crous, *sp. nov.* — MycoBank MB838013; Fig. 7

Etymology. Name reflects the location where it was collected, Golestan Province, Iran.

Typus. Iran, Golestan Province, on *Agropyron tauri*, 2011, *M. Razavi* (holotype CBS H-24388, cultures ex-type CPC 36217 = Pat-6 IR_6_1.1 = CBS 146871).

Conidiomata solitary, pycnidial, brown, globose, 200–350 µm diam, with central ostiole oozing saffron conidial masses; wall with 3–6 layers of pale brown *textura angularis. Conidiophores* reduced to conidiogenous cells lining the inner cavity. *Conidiogenous cells* hyaline, smooth, ampulliform, 5–10 × 4–5 µm, proliferating percurrently at apex. *Conidia* solitary, hyaline, smooth, guttulate, subcylindrical, straight to slightly curved, apex subobtuse, base truncate, 1.5–2 µm diam, (1–)3-septate, (22–)25–30(–35) × 2.5(–3) µm.

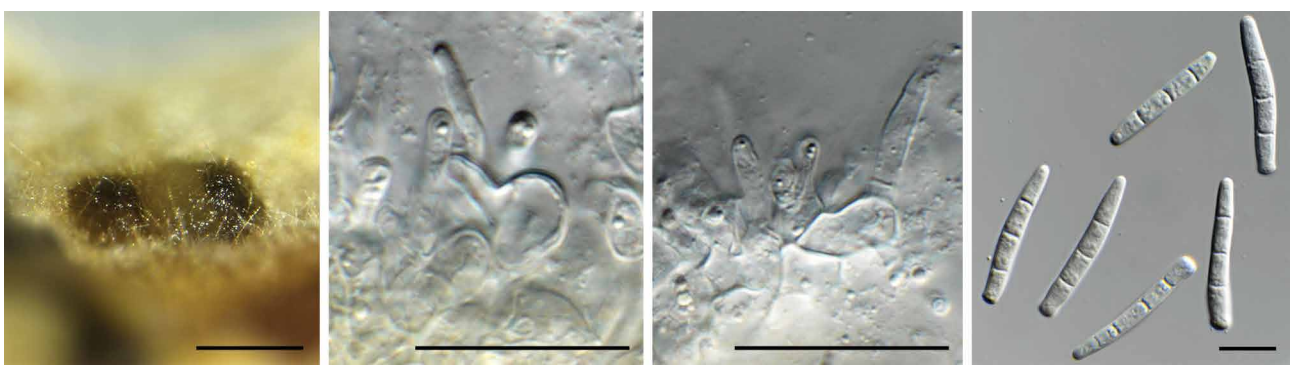

Fig. 6 *Parastagonospora dactylidigena* (CPC 36213). a. Conidiomata developing on PDA; b–c. conidiogenous cells giving rise to conidia; d. conidia. — Scale bars: a–c = 200 µm, all others = 10 µm.

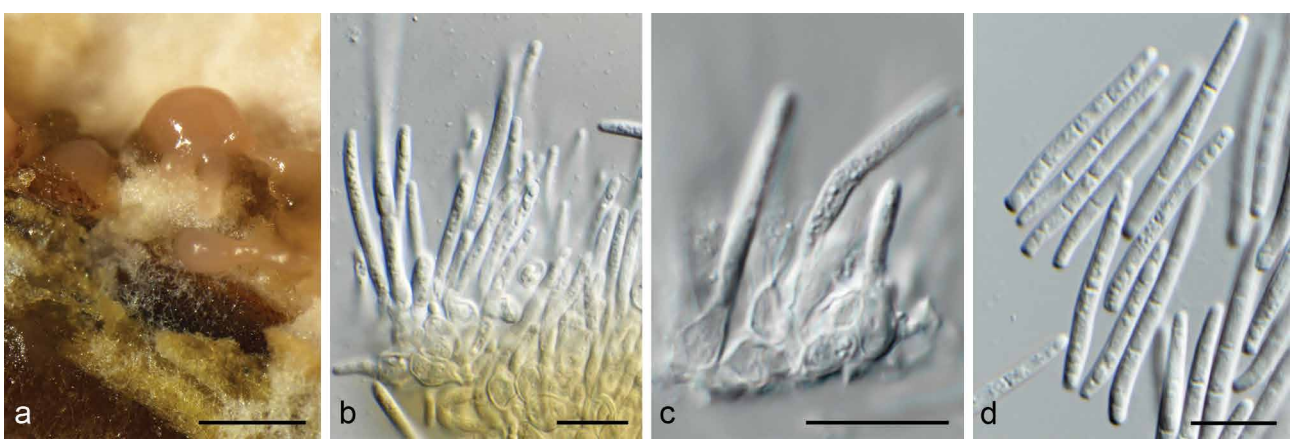

Fig. 7 *Parastagonospora golestanensis* (CPC 36217). a. Conidiomata developing on PDA; b–c. conidiogenous cells giving rise to conidia; d. conidia. — Scale bars: a = 350 µm, all others = 10 µm.

Culture characteristics — Colonies flat, spreading, reaching 60 mm diam after 2 wk, with abundant aerial mycelium, and even, lobate margins. On MEA surface saffron, reverse sienna; on PDA surface and reverse saffron; on OA surface saffron.

Notes — *Parastagonospora golestanensis* occurs on *Agropyron*, but has also been isolated from *Dactylis glomerata*. Morphologically, it is similar to taxa occurring in the *P. nodorum* complex, and these species are best distinguished based on DNA data.

Parastagonospora jasniorum B.A. McDonald, P.C. Brunner, Croll, D. Pereira & Crous, *sp. nov.* — MycoBank MB838014; Fig. 8

Etymology. Name reflects a condensation of Jasmine and Nicholas, the first names of the children of the senior author Patrick Brunner.

Typus. Iran, Golestan Province, near Aliabad-e-Katul, on infected glume of *Triticum aestivum*, June 2005, *M. Razavi* (holotype CBS H-24383, cultures ex-type CPC 36200 = P-2 IR_A1_3.1A = CBS 146866).

Ascocarps pseudothecial, solitary to aggregated, 120–170 µm diam, globose, brown, with central ostiole; wall of 3–6 layers of brown *textura angularis. Asci* 55–70 × 8–11 µm, bitunicate, short stipitate, straight to flexuous, subcylindrical, with well-defined apical chamber, 1–1.5 µm diam. *Pseudoparaphyses* hyaline, septate, hyphae-like, branched, septate, 2.5–3 µm diam. *Ascospores* bi- to tri-seriate, fusoid, pale brown, verruculose, widest in penultimate cell, 3-septate, not to slightly constricted at septa, (19–)21–22(–23) × (3.5–)4(–5) µm. *Conidiomata* 250–300 µm diam, dark brown to black, pycnidial, globose with central ostiole, exuding pale brown conidial mass; wall of 2–3 layers of brown *textura angularis. Conidiophores* reduced to conidiogenous cells lining the inner cavity. *Conidiogenous cells* phialidic, hyaline, smooth, aggregated, ampulliform, with percurrent proliferation at apex, 5–6 × 4–5 µm. *Conidia* pale brown, smooth, straight to flexuous, subcylindrical, guttulate, apical cell with slight taper to subobtuse apex, basal cell with slight taper to truncate hilum, 1.5–2 µm diam, (1–)3(–5)-septate, (22–)27–32(–35) × (2.5–)3 µm.

Cultural characteristics — Colonies covering dish in 2 wk at 25 °C in the dark, with moderate fluffy aerial mycelium and smooth, lobate margin. On MEA surface hazel with isabelline outer region, reverse cinnamon with patches of isabelline; on PDA surface and reverse honey; on OA surface honey with patches of hazel.

Notes — *Parastagonospora jasniorum* is distinguished from *P. nodorum* (conidia 0–3-septate) based on its conidial septation.

Parastagonospora nodorum (Berk.) Quaedvlieg et al., Stud. Mycol. 75: 363. 2013 — Fig. 9

Basionym. *Depazea nodorum* Berk., Gard. Chron., London: 601. 1845.
Synonyms. *Septoria nodorum* (Berk.) Berk., Gard. Chron., London: 601. 1845.
Stagonospora nodorum (Berk.) E. Castell. & Germano, Annali Fac. Sci. Agr. Univ. Torino 10: 71. 1977. [1975–1976].
Leptosphaeria nodorum E. Müll., Phytopath. J. 19: 409. 1952.
Phaeosphaeria nodorum (E. Müll.) Hedjar., Sydowia 22: 79. 1969 [1968].

Conidiomata solitary, pycnidial, brown, globose, 200–300 µm diam, with central ostiole, 10–15 µm diam, oozing hyaline conidial masses; wall with 3–6 layers of pale brown *textura angularis. Conidiophores* reduced to conidiogenous cells lining the inner cavity. *Conidiogenous cells* hyaline, smooth, globose to ampulliform, 5–7 × 4–6 µm, proliferating percurrently at apex. *Conidia* solitary, hyaline, smooth, guttulate, subcylindrical, straight to irregularly curved, apex subobtuse, base truncate, 1–3-septate, (11–)13–18(–28) × (2.5–)3(–3.5) µm.

Culture characteristics — Colonies flat, spreading, covering dish after 2 wk, with moderate aerial mycelium, and even, smooth margins. On MEA, PDA and OA surface pale olivaceous grey to olivaceous grey, reverse olivaceous grey.

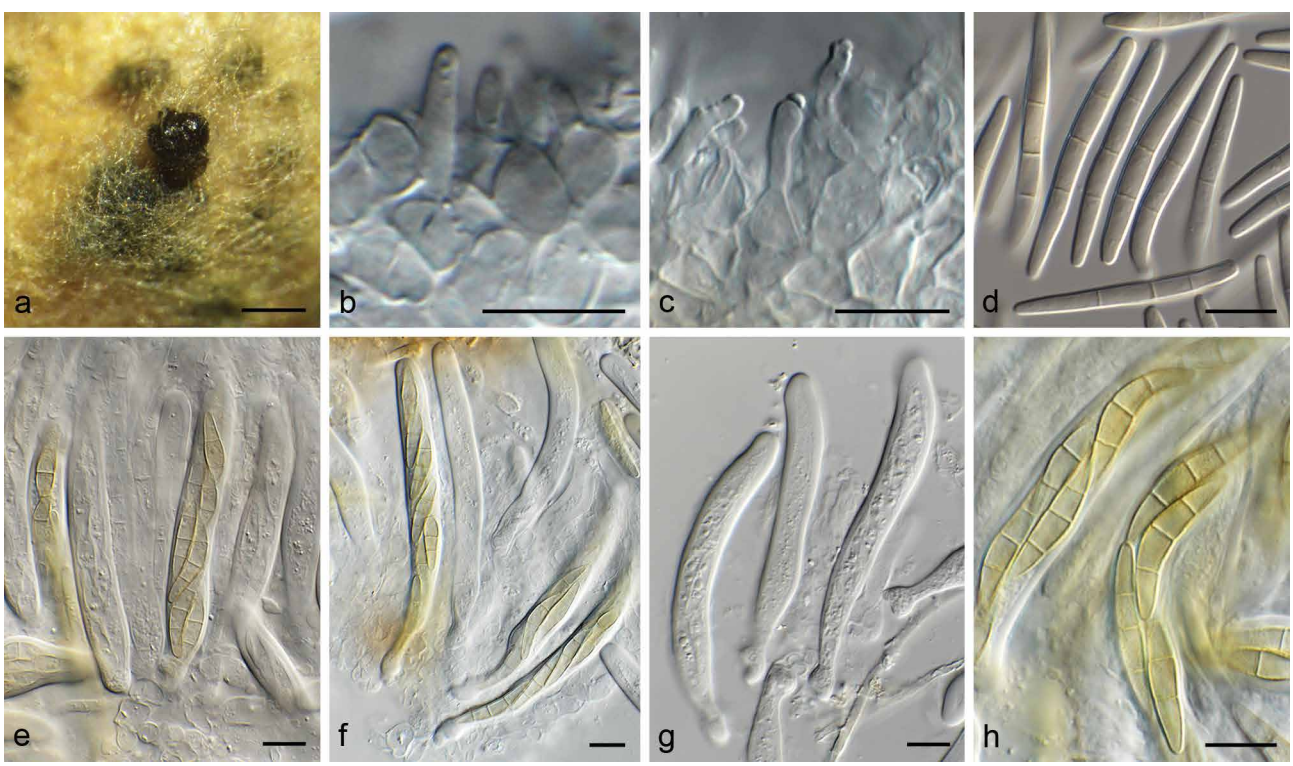

Fig. 8 *Parastagonospora jasniorum* (CPC 36200). a. Conidiomata developing on PDA; b–c. conidiogenous cells giving rise to conidia; d. conidia; e–h. asci and ascospores. — Scale bars: a = 300 µm, all others = 10 µm.

Material examined. Iran, Golestan Province, near Aliabad-e-Katul, on *Triticum aestivum*, June 2005, *M. Razavi* (neotype specimen designated here CBS H-24391, MBT394790, culture ex-neotype CPC 36202 = nodorum_IR_B2.1B = CBS 146873).

Notes — Bissett (1982) noted that conidia *in vivo* can be 1–3-septate, 13–28 × 2.8–4.6 (av. 19 × 3.6) µm in size, while Eyal et al. (1987) reported conidia to be 0–3-septate, 15–32 × 2–4 µm.

Parastagonospora nodorum is a common pathogen of *Triticum aestivum*, and occurs wherever this host is grown. This pathogen was originally described as *Depazea nodorum* from wheat collected in the UK, but no holotype specimen was indicated. This is rectified here, with the present reference strain (for which a full genome sequence is available) being designated as ex-neotype.

Parastagonospora pseudonodorum B.A. McDonald, P.C. Brunner, Croll, D. Pereira & Crous, *sp. nov.* — MycoBank MB838015; Fig. 10

Etymology. Name reflects its morphological similarity to *Parastagonospora nodorum*.

Typus. Iran, Golestan Province, on infected *Triticum aestivum*, 2010, *M. Razavi* (holotype CBS H-24384, cultures ex-type CPC 36208 = Pat-1 IR_5.2B = CBS 146867).

Conidiomata solitary, pycnidial, brown, globose, 200–350 µm diam, with central ostiole; wall with 3–6 layers of pale brown *textura angularis*. *Conidiophores* reduced to conidiogenous cells lining the inner cavity. *Conidiogenous cells* hyaline, smooth, ampulliform to subcylindrical, 4–9 × 4–6 µm, proliferating percurrently at apex. *Conidia* solitary, hyaline, smooth, guttulate, cylindrical, straight to slightly curved, apex subobtuse, base truncate, 2.5–3 µm diam, 3-septate, (27–)30–33(–36) × (2.5–)3(–3.5) µm.

Culture characteristics — Colonies spreading, covering dish after 2 wk, with moderate fluffy aerial mycelium, and even, lobate margins. On MEA surface saffron, reverse orange; on PDA surface and reverse saffron; on OA surface smoke grey.

Notes — *Parastagonospora pseudonodorum* coexists with *P. nodorum* on wheat, but is more often found on heads and seeds instead of on leaves. Morphologically the two species can be distinguished in that conidia of *P. pseudonodorum* are somewhat longer than those of *P. nodorum* (see above).

Parastagonospora stipae B.A. McDonald, P.C. Brunner, Croll, D. Pereira, Mordecai & Crous, *sp. nov.* — MycoBank MB838016; Fig. 11

Etymology. Name reflects the host genus it was isolated from, *Stipa*.

Typus. USA, California, Woodside, Jasper Ridge Biological Preserve, on *Stipa pulchra* (formerly *Nassella pulchra*), 2015, *E. Mordecai* and *E. Spear* (holotype CBS H-24389, cultures ex-type CPC 36223 = New-3 MORDECAI_1418 = CBS 146872).

Culture nearly sterile, with only a few conidiomata observed. *Conidiomata* solitary, pycnidial, dark brown, globose, 150–180 µm diam, with central, darker brown ostiole; wall with 3–6 layers of pale brown *textura angularis*. *Conidiophores* reduced to conidiogenous cells lining the inner cavity. *Conidiogenous cells* hyaline, smooth, ampulliform to subcylindrical, 5–6 × 3–4 µm, proliferating percurrently at apex. *Conidia* solitary, hyaline, smooth, guttulate, subcylindrical, straight to slightly curved, apex subobtuse, base truncate, 2 µm diam, 1-septate, (8–)10–13(–18) × (2.5–)3 µm.

Culture characteristics — Colonies flat, spreading, covering dish after 2 wk, with moderate aerial mycelium, and even, smooth margins. On MEA surface luteous, reverse sienna; on PDA surface and reverse sienna; on OA surface pale luteous.

Fig. 9 *Parastagonospora nodorum* (CPC 36202). a. Conidiomata developing on PDA; b. conidial cirrhus; c. conidiogenous cells giving rise to conidia; d. conidia. — Scale bars: a = 300 µm, all others = 10 µm.

Fig. 10 *Parastagonospora pseudonodorum* (CPC 36208). a. Conidiomata developing on PDA; b–c. conidiogenous cells giving rise to conidia; d. conidia. — Scale bars: a = 350 µm, all others = 10 µm.

Notes — *Parastagonospora stipae* occurs on *Stipa*, and is distinguished from taxa in the *P. nodorum* complex based on its smaller conidia.

Parastagonospora zildae B.A. McDonald, P.C. Brunner, Croll, D. Pereira & Crous, *sp. nov.* — MycoBank MB838017; Fig. 12

Etymology. *zildae* = Named after Zilda, the first name of the mother of the co-author Danilo Pereira.

Typus. Iran, Golestan Province, near Aliabad-e-Katul, on infected glume of *Triticum aestivum*, June 2005, *M. Razavi* (holotype CBS H-24381, cultures ex-type CPC 36198 = P-1 IR_B4.2A = CBS 146864).

CPC 36198 = P-1 IR_B4.2A: *Ascocarps* pseudothecial, solitary to aggregated, erumpent, globose, dark brown, 200–250 µm diam; wall of 3–6 layers of brown *textura angularis*; ostiole central, 15–25 µm diam, not to slightly papillate. *Asci* 55–85 × 7–9 µm, bitunicate, subcylindrical, straight to slightly curved, short stipitate, 8-spored, with well-defined apical chamber, 1–1.5 µm diam. *Pseudoparaphyses* filiform, hyaline, septate, hyphae-like, unbranched, rarely anastomosing, 2–2.5 µm diam. *Ascospores* bi- to triseriate in asci, fusoid, guttulate, pale brown, smooth, widest in penultimate cell, becoming slightly constricted at septa with age, (24–)26–28(–32) × (3.5–)4 µm, 5–6-septate.

CPC 36221 = New-1 IR_C2.2A: *Ascocarps* pseudothecial, solitary, erumpent, globose, dark brown, 180–250 µm diam; wall of 3–6 layers of brown *textura angularis*; ostiole central, 15–25 µm diam, not to slightly papillate. *Asci* bitunicate, 65–85 × 8–11 µm, subcylindrical, straight to slightly curved, short stipitate, 8-spored, with well-defined apical chamber, 1.5–2 µm diam. *Pseudoparaphyses* filiform, hyaline, septate, hyphae-like, branched below, rarely anastomosing, 2–3 µm diam. *Ascospores* bi- to triseriate in asci, fusoid, guttulate, pale brown, smooth, widest in penultimate cell, becoming slightly constricted at septa with age, (24–)25–26(–28) × 4(–5) µm, 5(–6)-septate.

Cultural characteristics — Colonies covering dish after 2 wk at 25 °C in the dark, smooth, with even margin, and moderate to fluffy aerial mycelium. On MEA surface buff with patches

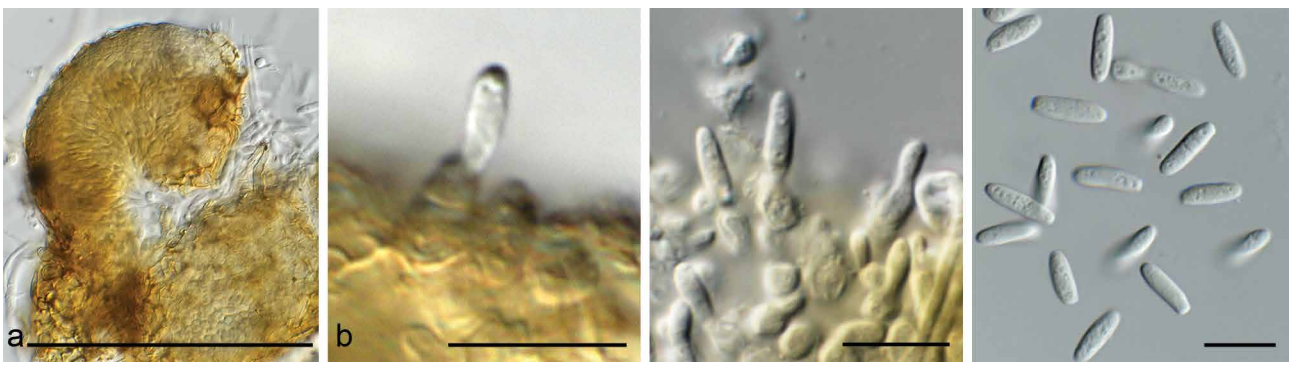

Fig. 11 *Parastagonospora stipae* (CPC 36223). a. Broken conidiomata with conidia; b–c. conidiogenous cells giving rise to conidia; d. conidia. — Scale bars: a = 200 µm, all others = 10 µm.

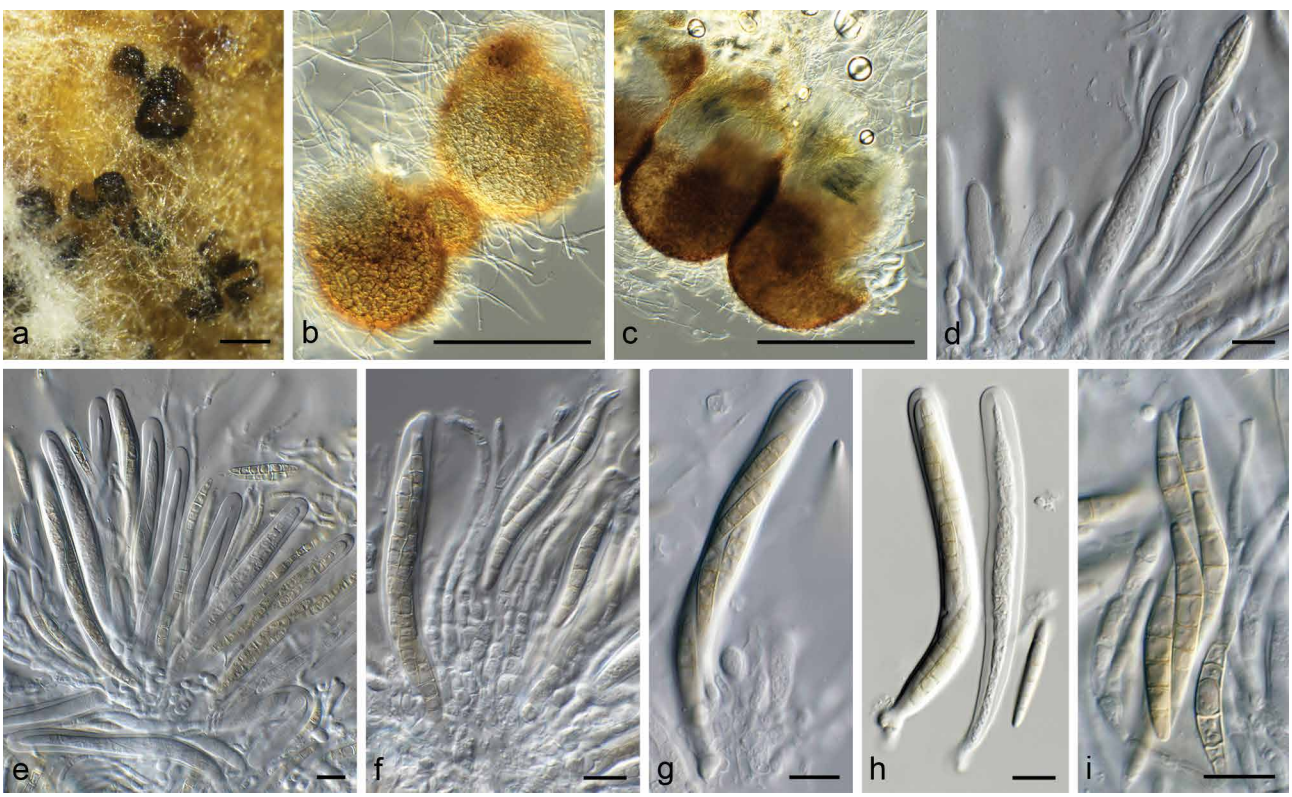

Fig. 12 *Parastagonospora zildae* (CPC 36198). a–c. Ascomata developing on PDA; d–h. asci, pseudoparaphyses and ascospores; i. ascospores. — Scale bars: a–c = 200 µm, all others = 10 µm.

of honey, reverse isabelline; on PDA surface pale olivaceous grey, reverse grey olivaceous; on OA surface grey olivaceous in centre, cinnamon in outer region.

Additional specimen examined. Iran, Golestan Province, near Aliabad-e-Katul, on infected glume of *Triticum aestivum*, June 2005, *M. Razavi* (CBS H-24382, cultures CPC 36221 = New-1 IR_C2.2A = CBS 146865).

Notes — Cultures of *P. zildae* only produced a sexual morph in culture, making a morphological comparison with asexual species difficult. Species such as *P. nodorum* do have a sexual morph (originally described as *Leptosphaeria nodorum*, ascospores 3-septate, 23–32 × 4–6 µm; Eyal et al. 1987), although this is not commonly observed.

DISCUSSION

Genome-scale sequence comparisons allowed us to differentiate several new species of *Parastagonospora* and determine their phylogenetic relationships. The highest species diversity was found in *Parastagonospora* collections from the Fertile Crescent, the region where wheat was domesticated, consistent with earlier hypotheses that the Fertile Crescent is the centre of origin for wheat-infecting *Parastagonospora* spp. We consider it noteworthy that five *Parastagonospora* species were found infecting wheat in Iran, but only two of these species (*P. nodorum* and *P. pseudonodorum*) are commonly found on wheat worldwide. This finding suggests that there is potential for other *Parastagonospora* species to 'escape' from the Fertile Crescent region and emerge as new pathogens on wheat in other regions. Both *P. nodorum* and *P. pseudonodorum* are known to infect seed, so it is likely that these pathogens were moved around the world on infected seed, but it remains unknown whether the other three *Parastagonospora* species found on wheat in Iran are also able to infect seed.

An earlier coalescent analysis of five genes suggested that the grass-infecting *Parastagonospora* species could be broadly separated into 'young' and 'old' species, with the youngest species including *P. pseudonodorum*, *P. golestanensis*, *P. nodorum* and *P. avenae* and the older species including *P. zildae* and *P. jasniorum* (McDonald et al. 2012). The new genome-scale analyses largely supported this hypothesis, with the younger species showing shorter branch lengths consistent with more recent speciation events while the older species showed deeper divergences consistent with much earlier speciation events. We speculate that the young *Parastagonospora* species emerged mainly in the Fertile Crescent as a result of selection to become specialized to infect agricultural crops (e.g., wheat, oats and barley) and the weedy grasses often associated with these crops. The most parsimonious scenario is that the speciation events coincide with the onset of agriculture in the region, similar to findings on the emergence of the wheat pathogen *Zymoseptoria tritici* (syn. *Mycosphaerella graminicola*) (Stukenbrock et al. 2007a).

An earlier study (McDonald et al. 2012) that analyzed sequences from five genes in more than 350 global *Parastagonospora* strains identified 14 strains that appeared to be hybrids because they carried alleles that were otherwise exclusive to either *P. nodorum* or *P. pseudonodorum* (formerly *Pat-1*). The complete genome sequences reported here for three of these strains showed no evidence for hybridization, with each isolate falling clearly into either the *P. nodorum* (CASSILS) or the *P. pseudonodorum* (JANSEN4, HARTNEY) clade. Genomes of true hybrids are expected to occupy an intermediate phylogenetic position compared to the parental species. Future analyses of the genomic datasets should focus on identifying rare recombination events that can lead to gene introgression among species. We expect that such events could have occurred among *P. pseudonodorum* and *P. nodorum*, which could also explain how *P. pseudonodorum* acquired the *ToxA*, *Tox1* and *Tox3* genes from *P. nodorum* (McDonald et al. 2013, Ghaderi et al. 2020). The preponderance of *P. pseudonodorum* on grain and ears suggests that this species exhibits host-tissue specialization, with a preference to infect ears. In comparison, *P. nodorum* is typically found on both leaves and ears.

Overall, our data is consistent with the hypothesis that *P. nodorum* originated as a pathogen of wild grasses in the Fertile Crescent, then emerged as a wheat pathogen via host-tracking during the domestication of wheat in the same region. It is likely that *P. nodorum* became distributed globally via movement of infected wheat seed during the global spread of wheat agriculture that included North America. The discovery in California of *Stipa* pathogens that appeared closely related to *P. nodorum* is also consistent with a 'spill-back' as a possible source for this population infecting wild grasses. While the tree based on five AFTOL genes provides some weak support for the spill-back hypothesis, the tree based on four AFTOL genes does not. Therefore, we do not find definitive evidence that *P. stipae* was most closely associated with *P. nodorum* or consistently shared a most recent common ancestor with *P. nodorum*. Genome sequences from *P. stipae* will be needed to further test the spillback hypothesis.

Acknowledgements EAM was supported by the National Science Foundation (DEB-1518681 and DEB-2011147, and the Fogarty International Center), the National Institutes of Health (R35GM133439), the Jasper Ridge Biological Preserve Kennedy Endowment, and the Terman Award. The senior author, Patrick C. Brunner, initiated and led this project but died of cancer before the work could be completed. We dedicate this paper to him and his family.

REFERENCES

Bankevich A, Nurk S, Antipov D, et al. 2012. SPAdes: a new genome assembly algorithm and its applications to single-cell sequencing. Journal of Computational Biology 19: 455–477.

Bissett J. 1982. Stagonospora avenae. Fungi Canadenses No. 239. National Mycological Herbarium, Biosystematics Research Institute Agriculture Canada, Ottawa.

Brahmanage RS, Dayarathne MC, Wanasinghe DN, et al. 2020. Taxonomic novelties of saprobic Pleosporales from selected dicotyledons and grasses. Mycosphere 11: 2481–2541.

Crous PW, Verkley GJM, Groenewald JZ, et al. (eds). 2019. Fungal Biodiversity. Westerdijk Laboratory Manual Series 1: 1–425. Westerdijk Fungal Biodiversity Institute, Utrecht, The Netherlands.

Cunfer B, Ueng P. 1999. Taxonomy and identification of Septoria and Stagonospora species on small-grain cereals. Annual Review of Phytopathology 37: 267–284.

Dobin A, Davis CA, Schlesinger F, et al. 2013. STAR: ultrafast universal RNA-seq aligner. Bioinformatics 29: 15–21.

Emms DM, Kelly S. 2019. OrthoFinder: phylogenetic orthology inference for comparative genomics. Genome Biology 20: 238.

Eyal Z, Scharen AL, Prescott JM, et al. 1987. The Septoria diseases of wheat: concepts and methods of disease management. Mexico, CIMMYT.

Ghaderi F, Sharifnabi B, Javan-Nikkhah M, et al. 2020. SnToxA, SnTox1 and SnTox3 originated in Parastagonospora nodorum in the Fertile Crescent. Plant Pathology 69: 1482–1491.

Goonasekara I, Erio C, Bulgakov T, et al. 2019. Two novel species of Parastagonospora (Phaeosphaeriaceae, Pleosporales) on grasses from Italy and Russia. Asian Journal of Mycology 2: 170–182.

Gurevich A, Saveliev V, Vyahhi N, et al. 2013. QUAST: quality assessment tool for genome assemblies. Bioinformatics 29: 1072–1075.

Hane JK, Lowe RGT, Solomon PS, et al. 2007. Dothideomycete plant interactions illuminated by genome sequencing and EST analysis of the wheat pathogen Stagonospora nodorum. The Plant Cell 19: 3347–3368.

Hoff KJ, Lomsadze A, Borodovsky M, et al. 2019. Whole-genome annotation with BRAKER. Methods in Molecular Biology 1962: 65–95.

Jones DAB, John E, Rybak K, et al. 2019. A specific fungal transcription factor controls effector gene expression and orchestrates the establishment of the necrotrophic pathogen lifestyle on wheat. Scientific Reports 9: 15884. https://doi.org/10.1038/s41598-019-52444-7.

Katoh K, Rozewicki J, Yamada KD. 2019. MAFFT online service: multiple sequence alignment, interactive sequence choice and visualization. Briefings in Bioinformatics 20: 1160–1166.
Katoh K, Standley DM. 2013. MAFFT multiple sequence alignment software version 7: improvements in performance and usability. Molecular Biology and Evolution 30: 772–780.
Keller SM, McDermott JM, Pettway RE, et al. 1997. Gene flow and sexual reproduction in the wheat glume blotch pathogen Phaeosphaeria nodorum (anamorph Stagonospora nodorum). Phytopathology 87: 353–358.
Kelly DW, Paterson RA, Townsend CR, et al. 2009. Parasite spillback: a neglected concept in invasion ecology? Ecology 90: 2047–2056.
Kiros-Meles A, Gomez D, McDonald BA, et al. 2011. Invasion of Rhynchosporium commune onto wild barley in the Middle East. Biological Invasions 13: 321–330.
Kozlov AM, Darriba D, Flouri T, et al. 2019. RAxML-NG: a fast, scalable and user-friendly tool for maximum likelihood phylogenetic inference. Bioinformatics 35: 4453–4455.
Li GJ, Hyde KD, Zhao RL, et al. 2016. Fungal diversity notes 253–366: taxonomic and phylogenetic contributions to fungal taxa. Fungal Diversity 78: 1–237.
Li WJ, Bhat DJ, Camporesi E, et al. 2015. New asexual morph taxa in Phaeosphaeriaceae. Mycosphere 6: 681–708.
Malkus A, Reszka E, Chang C-J, et al. 2005. Sequence diversity of β-tubulin (tubA) gene in Phaeosphaeria nodorum and P. avenaria. FEMS Microbiology Letters 249: 49–56. https://doi.org/10.1016/j.femsle.2005.05.049.
Marin-Felix Y, Hernández-Restrepo M, Iturrieta-González I, et al. 2019. Genera of phytopathogenic fungi: GOPHY 3. Studies in Mycology 94: 1–124.
Martin SI, Cooke BM. 1979. Effect of wheat and barley hosts on pathogenicity and cultural behaviour of barley and wheat isolates of Septoria nodorum. Transactions of the British Mycological Society 72: 219–224.
McDonald MC, Oliver RP, Friesen TL, et al. 2013. Global diversity and distribution of three necrotrophic effectors in Phaeosphaeria nodorum and related species. New Phytologist 199: 241–251.
McDonald MC, Razavi M, Friesen TL, et al. 2012. Phylogenetic and population genetic analysis of Phaeosphaeria nodorum and its close relative indicate cryptic species and an origin in the Fertile Crescent. Fungal Genetics and Biology 49: 882–895.
Osbourn A, Scott P, Caten C. 1986. The effects of host passaging on the adaptation of Septoria nodorum to wheat or barley. Plant Pathology 35: 135–145.
Pereira D, Brunner PC, McDonald BA. 2020a. Natural selection drives population divergence for local adaptation in a wheat pathogen. Fungal Genetics and Biology 141: 103398.
Pereira D, McDonald BA, Brunner PC. 2017. Mutations in the CYP51 gene reduce DMI sensitivity in Parastagonospora nodorum populations in Europe and China. Pest Management Science 73: 1503–1510.
Pereira D, McDonald BA, Croll D. 2020b. The genetic architecture of emerging fungicide resistance in populations of a global wheat pathogen. Genome Biology and Evolution 12 (12): 2231–2244. https://doi.org/10.1093/gbe/evaa203.
Pereira D, Oggenfuss U, McDonald BA, et al. 2020c. The population genomics of transposable element activation in the highly repressive genome of an agricultural pathogen. bioRxiv. https://doi.org/10.1101/2020.11.12.379651.
Rayner RW. 1970. A Mycological Colour Chart. Kew, Commonwealth Mycological Institute, Kew, UK.
Richards JK, Stukenbrock EH, Carpenter J, et al. 2019. Local adaptation drives the diversification of effectors in the fungal wheat pathogen Parastagonospora nodorum in the United States. PLoS Genetics 15: e1008223.
Salamini F, Ozkan H, Brandolini A, et al. 2002. Genetics and geography of wild cereal domestication in the Near East. Nature Reviews Genetics 3: 429–441.
Shaw DE. 1957a. Studies on Leptosphaeria avenaria f. sp. avenaria. Canadian Journal of Botany 35: 97–112.
Shaw DE. 1957b. Studies on Leptosphaeria avenaria f. sp. triticea on cereals and grasses. Canadian Journal of Botany 35: 113–118.
Sommerhalder RJ, McDonald BA, Zhan J. 2007. Concordant evolution of mitochondrial and nuclear genomes in the wheat pathogen Phaeosphaeria nodorum. Fungal Genetics and Biology 44: 764–772.
Spear ER, Mordecai EA. 2018. Foliar pathogens of California grasses are multi-host and spatially widespread: implications for grassland diversity. Ecology 99: 2250–2259.
Stamatakis A. 2014. RAxML version 8: a tool for phylogenetic analysis and post-analysis of large phylogenies. Bioinformatics 30: 1312–1313.
Stanke M, Morgenstern B. 2005. AUGUSTUS: a web server for gene prediction in eukaryotes that allows user-defined constraints. Nucleic Acids Research 33 (Web Server issue): W465–7. https://doi.org/ 10.1093/nar/gki458.
Stukenbrock EH, Banke S, Javan-Nikkhah M, et al. 2007a. Origin and domestication of the fungal wheat pathogen Mycosphaerella graminicola via sympatric speciation. Molecular Biology and Evolution 24: 398–411.
Stukenbrock EH, Banke S, McDonald BA. 2006. Global migration patterns in the fungal wheat pathogen Phaeosphaeria nodorum. Molecular Ecology 15: 2895–2904.
Stukenbrock EH, McDonald BA. 2007b. Geographic variation and positive diversifying selection in the host specific toxin SnToxA. Molecular Plant Pathology 8: 321–332.
Stukenbrock EH, McDonald BA. 2008. The origins of plant pathogens in agro-ecosystems. Annual Review of Phytopathology 46: 75–100.
Syme RA, Tan K-C, Rybak K, et al. 2018. Pan-Parastagonospora comparative genome analysis-effector prediction and genome evolution. Genome Biology and Evolution 10: 2443–2457.
Thambugala KM, Wanasinghe DN, Phillips AJL, et al. 2017. Mycosphere notes 1–50: Grass (Poaceae) inhabiting Dothideomycetes. Mycosphere 8: 697–796.
Ueng PP, Chen W. 1994. Genetic differentiation between Phaeosphaeria nodorum and P. avenaria using restriction fragment length polymorphisms. Phytopathology 84: 800–806.
Ueng PP, Cunfer B, Alano A, et al. 1995. Correlation between molecular and biological characters in identifying the wheat and barley biotypes of Stagonospora nodorum. Phytopathology 85: 44–52.
Ueng PP, Subramaniam K, Chen W, et al. 1998. Intraspecific genetic variation of Stagonospora avenae and its differentiation from S. nodorum. Mycological Research 102: 607–614.
Untergasser A, Cutcutache I, Koressaar T, et al. 2012. Primer3--new capabilities and interfaces. Nucleic Acids Research 40: e115.
Yu G. 2020. Using ggtree to visualize data on tree-like structures. Current Protocols in Bioinformatics 69: e96.

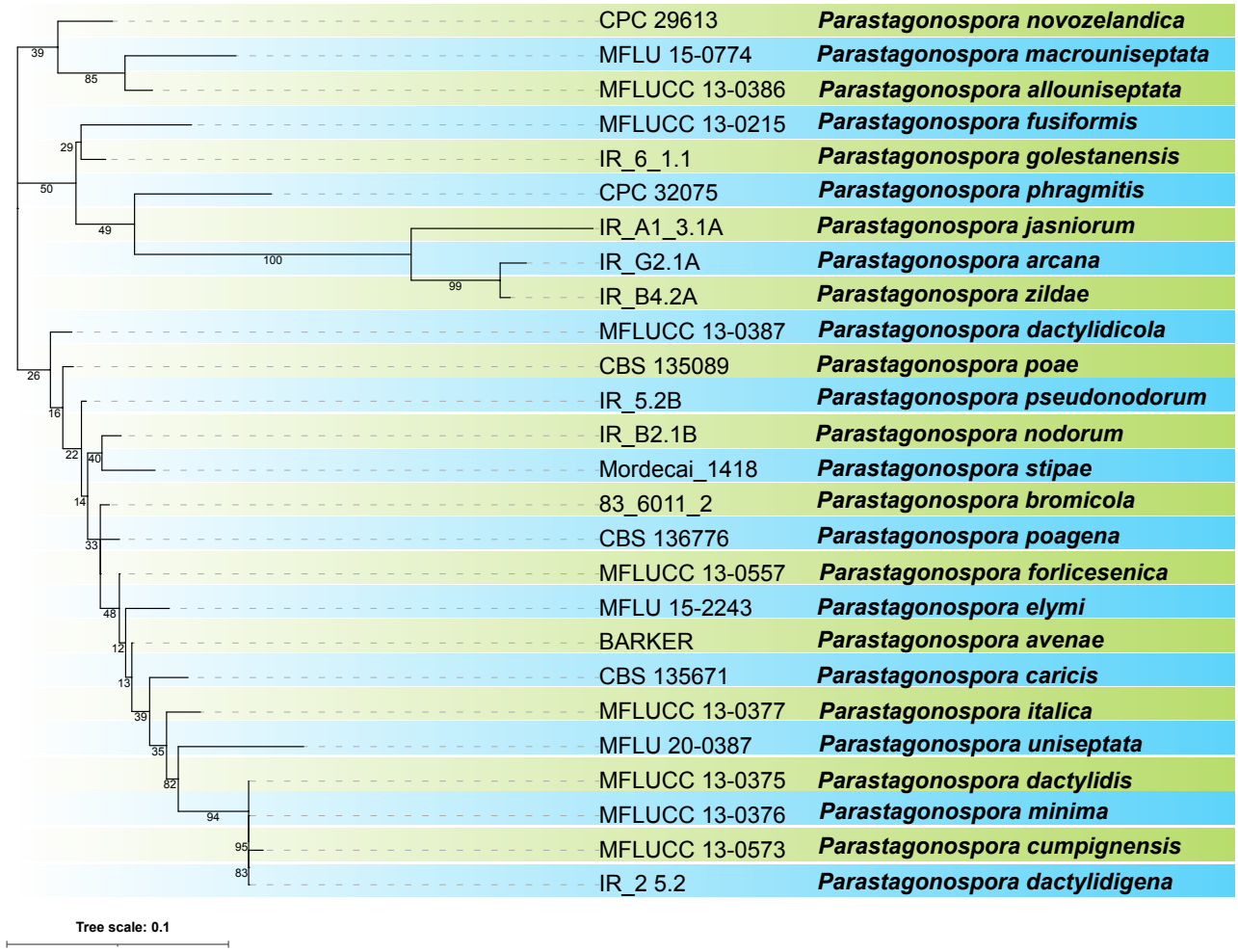

Appendix Maximum likelihood phylogenetic tree based on ITS sequences of 26 known *Parastagonospora* species. Additional ITS sequences were obtained from Goonasekara et al. (2019), Marin-Felix et al. (2019) and Brahmanage et al. (2020).